

3-2004

# Microwave Radiation Force on a Parallel-Plate Resonator

Sergey N. Makarov

Worcester Polytechnic Institute, makarov@wpi.edu

S. Kulkarni

Follow this and additional works at: <https://digitalcommons.wpi.edu/electricalcomputerengineering-pubs>



Part of the [Electrical and Computer Engineering Commons](#)

---

## Suggested Citation

Makarov, Sergey N. , Kulkarni, S. (2004). Microwave Radiation Force on a Parallel-Plate Resonator. *Applied Physics Letters*, 84(9), 1600-1602.

Retrieved from: <https://digitalcommons.wpi.edu/electricalcomputerengineering-pubs/15>

This Article is brought to you for free and open access by the Department of Electrical and Computer Engineering at Digital WPI. It has been accepted for inclusion in Electrical & Computer Engineering Faculty Publications by an authorized administrator of Digital WPI. For more information, please contact [digitalwpi@wpi.edu](mailto:digitalwpi@wpi.edu).

## Microwave radiation force on a parallel-plate resonator

S. Makarov<sup>a)</sup> and S. Kulkarni

Department of Electrical and Computer Engineering, Worcester Polytechnic Institute, 100 Institute Road, Worcester, Massachusetts 01609-2280

(Received 27 October 2003; accepted 3 January 2004)

A simulation method is proposed and tested in order to determine the radiation force on metal targets whose size is comparable to wavelength. The method is based on the method of moments solution of the electric-field integral equation, accurate calculation of the near field, and removal of the self-interaction terms responsible for the pinch effect. The method is used to determine the local force distribution for a parallel-plate metal resonator. It is observed that, at the resonance, the individual metal plates may experience large force densities, despite the fact that the net radiation force on the resonator still remains very small. A potential use of this observation is discussed, which is directed toward possible excitation of acoustic vibrations. © 2004 American Institute of Physics. [DOI: 10.1063/1.1650901]

The radiation forces and torques of a laser beam on small transparent dielectric objects were investigated long ago, both theoretically<sup>1</sup> and experimentally.<sup>2,3</sup> Recent (macro) applications of the optical radiation force include laser or optical tweezers<sup>4,5</sup> and optically driven micro electro mechanical systems.<sup>6,7</sup> The advantage of applying the laser beam to a dielectric is a relatively high intensity of the primary field as well as a relatively low absorption loss in the transparent dielectric.

The radiation forces on metal targets have received little attention. One portion of work was devoted to very small metal particles.<sup>8</sup> On the other hand, one should perhaps mention limited research related to solar radiation pressure on satellites.<sup>9,10</sup> In that research, the radiation pressure is usually estimated using the basic high-frequency formula  $p = (1 + r)J/c$ ,<sup>11</sup> where  $J$  is the field intensity,  $c$  is the speed of light, and  $r$  is the reflection coefficient.

The finite metal targets are not very well suited for applying the laser beams, primarily due to large absorption. However, the present letter will show that they potentially may experience significant *bending* radiation force effects at microwave frequencies, when the target is a resonator. The present letter will investigate the radiation force on a rectangular plate of infinitesimally small thickness, and a parallel-plate, electrically thin resonator at different  $Q$ . The plate size/wavelength ratio varies from 1/5 to 5.

The investigation is based on numerical simulation. Full-wave simulation using a three-dimensional version of the method of moments (MoM) solver for electric-field integral equation (EFIE) is employed. The scattered near field is accurately calculated in the vicinity of the surface grid. The numerical results are tested by comparison with Ansoft HFSS v. 9.0 (near field) and by running self-convergence tests for the radiation force.

The MoM formulation (metal scatterer) is rather standard and utilizes the mixed-potential approach to EFIE and the RWG basis functions.<sup>12,13</sup> We use the symmetric impedance matrix, which allows for a faster speed and larger memory storage. This is critical for the present large and lengthy computations in the frequency domain. The double

surface integrals are calculated using the Gaussian formulas of the fifth degree of accuracy.<sup>14</sup> All singular portions of self-integrals are found analytically, using the closed-form solutions given in Ref. 15. Factorization of the symmetric impedance matrix is done using the double-precision simple driver ZSYSV of the LAPACK library<sup>16</sup> for symmetric complex matrixes.

The total Lorentz force density on the surface current and charge distribution on a metal surface is given by (see, for example Ref. 17)

$$\mathbf{f} = \frac{1}{2} \text{Re}(\mathbf{J}_S \times \mathbf{B}^*) + \frac{1}{2} \text{Re}(\sigma_S \mathbf{E}^*), \quad \mathbf{B} = \mu_0 \mathbf{H}, \quad (1)$$

where  $\mathbf{E} = \mathbf{E}^s + \mathbf{E}^i$ ,  $\mathbf{H} = \mathbf{H}^s + \mathbf{H}^i$ , and index  $i$  denotes the incident field. The scattered fields  $\mathbf{E}^s$ ,  $\mathbf{H}^s$  are found numerically using already known current and charge densities  $\mathbf{J}_S$  and  $\sigma_S$ , respectively, solutions of the MoM equations. The total Lorentz force  $\mathbf{F}$  on a (open) metal surface  $S$  is given by

$$\mathbf{F} = \int_S \mathbf{f}(\mathbf{r}) ds. \quad (2)$$

For any small triangular patch on the metal surface, Eq. (2) contains a self-term that describes the interaction of the patch current and charge with the self-induced magnetic and electric fields. This effect cannot be described in terms of the model of an infinitesimally thin metal sheet (EFIE). The self-induced magnetic and electric fields are discontinuous on the sheet boundary so that Eq. (2) becomes meaningless. It is, however, well known that the interaction with the self-induced magnetic field in a volume conductor creates the pinch effect, in which the metal sheet is squeezed in transversal direction but does not experience any net force. The pinch force is thus of no interest for the present problem. The charge interaction with the self-induced electric field might also contribute to the pinch force. Thus, the following assumption is made when finding the force in Eq. (2). For any small triangular patch on the metal surface, Eq. (2) will ignore its own contribution to the fields  $\mathbf{E}^s$ ,  $\mathbf{H}^s$ , but will take into account contributions of all other patches.

The net radiation force on a single square metal plate at normal incidence [Fig. 1(a)] is found in Fig. 1(b). The plate mesh has  $60 \times 60$  rectangles (10 680 unknowns), which allows us to cover higher frequencies with up to five wave-

<sup>a)</sup>Electronic mail: makarov@wpi.edu

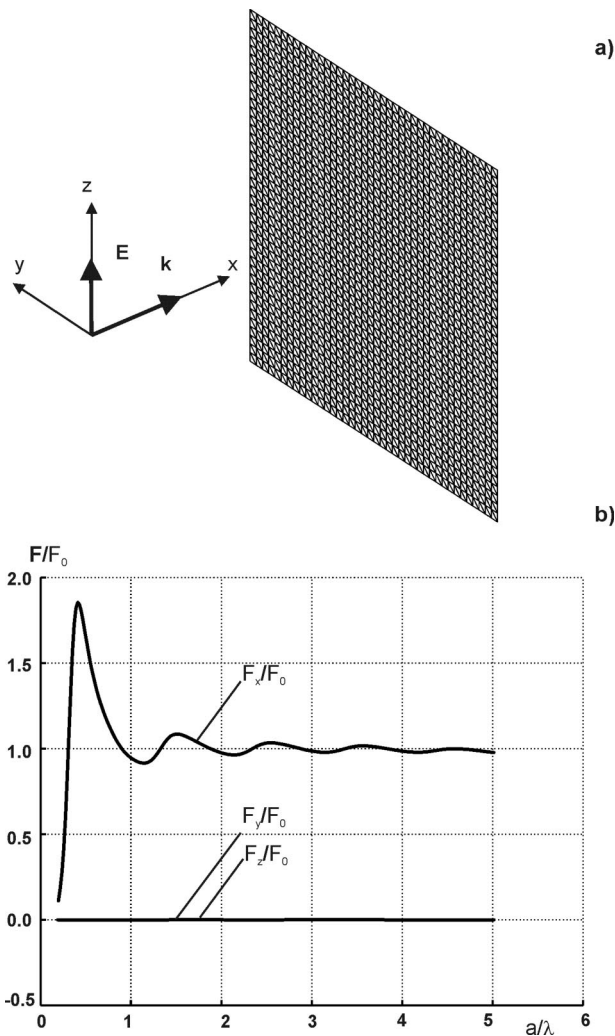


FIG. 1. (a) Geometry of incident signal for the single plate and (b) net radiation force as a function of the plate size/wavelength ratio. The original (simulation) plate mesh had  $60 \times 60$  rectangles (10 680 unknowns); 250 frequency steps are employed to cover the entire domain of  $a/\lambda$ .

lengths along the plate dimension  $a$ . Figure 1(b) shows three components of the total radiation force  $\mathbf{F}$  on the plate as functions of the ratio  $a/\lambda$ . The total force is normalized to its high-frequency limit  $F_0 = 2a^2J/c$ , where  $J$  is the intensity of the incident signal. One can see that the axial force  $F_x$  asymptotically tends to  $2a^2J/c$  at higher frequencies. At lower frequencies and, especially close to the first resonance, the force values appear to be somewhat higher than the high-frequency limit. The components  $F_y, F_z$  are at least 100 times smaller than  $F_x$ , as they should be for reasons of symmetry. In addition, the magnetic (Lorentz) component of the force in Eq. (1) clearly dominates as it follows from the solution analysis.

The scattering analysis of parallel-plate resonators has been among the first to be carried out by computer techniques about 40 years ago.<sup>18</sup> Eigenmode charts are available for basic resonator shapes.<sup>19,20</sup> However, the data on the radiation force or torque has not yet been reported.

The net radiation force on a parallel-plate resonator [Fig. 2(a)] is found in Fig. 2(b), in the vicinity of the first resonance (TM). The distance between plates  $d$  is 15% of the plate size  $a$ . The behavior of the net force is relatively smooth close to the resonance. The opposite situation, how-

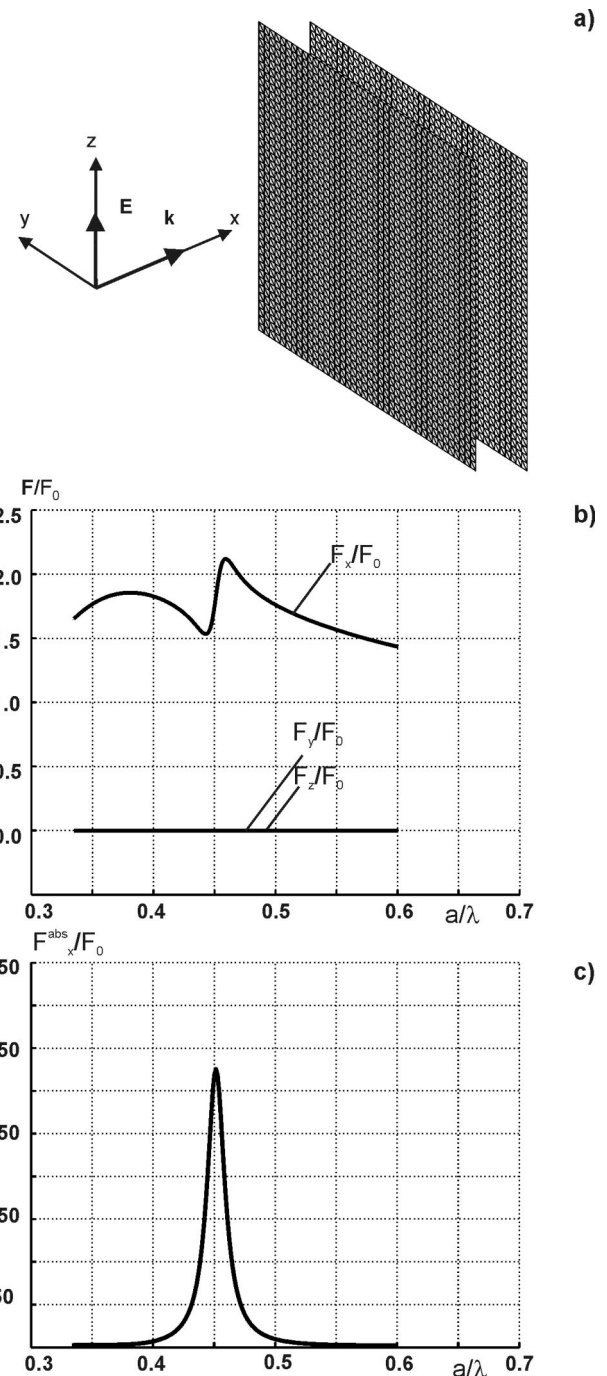


FIG. 2. (a) Geometry of the incident signal for the air-filled parallel-plate resonator; (b) net radiation force as a function of the plate size/wavelength ratio; and (c) magnitude of the force density integrated over the surface area. The original (simulation) mesh is a combination of two  $40 \times 40$  plate meshes (9440 unknowns).

ever, occurs if we consider the absolute value (magnitude) of the force density and then integrate the result over the surface area. Figure 2(c) shows the result for

$$F_x^{\text{abs}} = \int_S |f_x(\mathbf{r})| ds. \quad (3)$$

One can see that  $F_x^{\text{abs}}$  at the resonance is nearly 325 times the high-frequency limit  $F_0$ . The absolute force on a single plate is approximately one-half of this value.

To understand why  $F_x^{\text{abs}}$  is so different from the net force, we plotted the local force distribution. In Fig. 3(a), the surface shading indicates the surface value of the local force

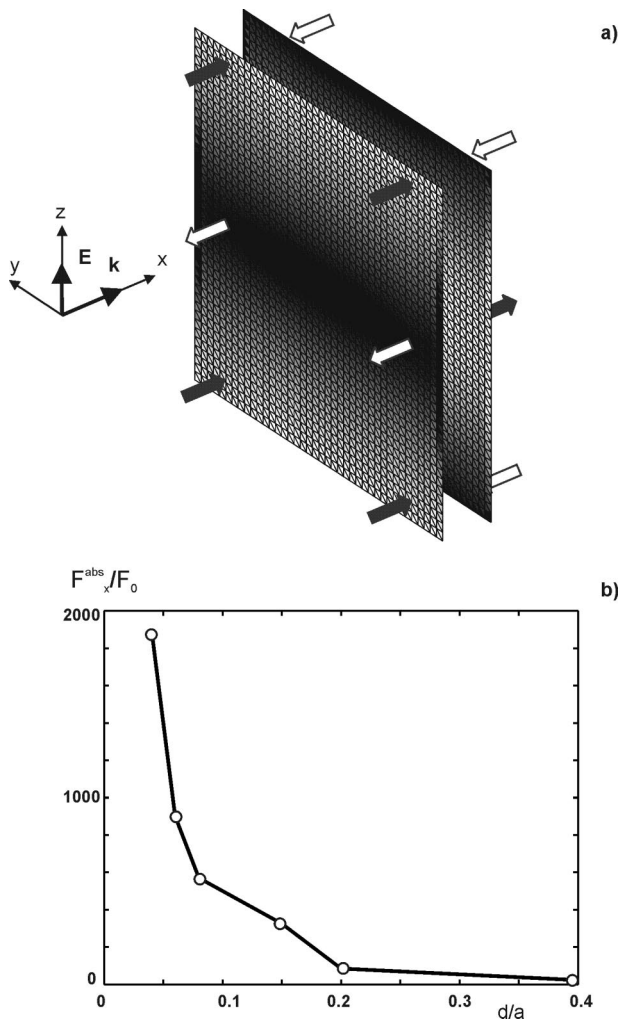


FIG. 3. (a) Force density distribution for the parallel-plate resonator with  $d/a=0.15$  at the first resonance. The surface gray scale extends from black (maximum force density in the direction of the negative  $x$  axis) to white (maximum force density in the direction of the positive  $x$  axis) and (b) magnitude of the force density integrated over the surface area  $F_x^{\text{abs}}$  for different ratios of  $d/a$  at the first resonance.

density  $f_x(\mathbf{r})$ , for the same resonator with  $d/a=0.15$ . The white color corresponds to positively directed force density (along the  $x$  axis), whereas the black color indicates the opposite direction. The local force density becomes very high at the resonance. Integrally, however, the forces cancel each other. This cancellation takes place not only between two plates but also for every individual plate. The net force  $F_x$  on a single plate was found to be about  $25F_0$  for the front plate and about  $24F_0$  for the second plate. Compared to the previous value of  $325F_0$ , this indicates almost perfect cancellation for an individual plate. It was also found that it is the contribution of the electric component of the force (insignificant for single plate) that is responsible for such a cancellation.

Similar results were observed for different plate size/resonator thickness ratios equal to  $d/a=0.04, 0.06, 0.08, 0.15, 0.20$ , and  $0.40$ . Figure 3(b) shows the maximum of  $F_x^{\text{abs}}$  at the resonance as a function of plate spacing. One can see that  $F_x^{\text{abs}}$  may be as high as  $2000F_0$  and tends to increase when the distance between plates decreases ( $Q$  of the resonator increases).

In conclusion, we discuss a possibility to use the ob-

tained force distribution in order to directly excite an acoustic mode in a parallel-plate resonator. The force density distribution shown in Fig. 3(a) creates a lateral surface loading  $p(y,z)=f_x(y,z)$  of a single plate. This loading is the source of plate bending, which is described by the lateral deflection  $w(y,z)$ . When the incident signal is amplitude modulated, plate loading becomes a function of time:  $p(y,z,t)$ . Alternatively, the incident signal may be frequency modulated. In that case, a deviation in frequency leads to detuning the parallel-plate resonator, which also implies a time-varying loading  $p(y,z,t)$ .

The time-varying loading  $p(y,z,t)$  excites flexural vibrations of a single plate that are governed by the well-known thin-plate equation (see, for example, Ref. 21, p. 210). This equation is subject to boundary conditions that may be defined from a possible experimental arrangement. For a rough estimate, we will use the average work done by the lateral surface loading (see Ref. 22, p. 90):

$$W^i = \frac{1}{2} \int_{S_i} \overline{p(y,z,t) \cdot w(y,z,t)} ds; \quad i=1,2, \quad (4)$$

where the overbar denotes time averaging (over the acoustic period) and  $i$  is the plate number. When the structure in Fig. 3(a) experiences an acoustic resonance, the local lateral deflection may be approximately assumed to be proportional to the local lateral pressure. The average work thus becomes proportional to the integral of the squared component of the local axial force. This could lead to an even more dramatic dependency of the delivered acoustic power on the  $Q$  of the resonator, compared to the dependency shown in Fig. 3(b).

<sup>1</sup>J. P. Barton, D. R. Alexander, and S. A. Schaub, *J. Appl. Phys.* **66**, 4594 (1989).

<sup>2</sup>A. Ashkin, *Phys. Rev. Lett.* **24**, 156 (1970).

<sup>3</sup>A. Ashkin, *IEEE J. Sel. Top. Quantum Electron.* **6**, 841 (2000).

<sup>4</sup>Y. Nahmias and D. J. Odde, *IEEE J. Quantum Electron.* **38**, 131 (2002).

<sup>5</sup>A. B. Nemet, Y. Shabtai, and M. Cronin-Golomb, *Opt. Lett.* **27**, 264 (2002).

<sup>6</sup>W. L. Collett, C. A. Ventrice, and S. M. Mahajan, *Appl. Phys. Lett.* **82**, 2730 (2003).

<sup>7</sup>E. Higurashi, O. Ohguchi, T. Tamamura, and H. Ukita, *J. Appl. Phys.* **82**, 2773 (1997).

<sup>8</sup>K. Svoboda and S. M. Block, *Opt. Lett.* **19**, 930 (1994).

<sup>9</sup>S. N. Singh, *IEEE Trans. Aerosp. Electron. Syst.* **32**, 732 (1996).

<sup>10</sup>R. Venkatachalam, *IEEE Trans. Aerosp. Electron. Syst.* **29**, 1164 (1993).

<sup>11</sup>P. N. Lebedev, *Ann. Phys. (Munich)* **6**, 433 (1901).

<sup>12</sup>A. F. Peterson, S. L. Ray, and R. Mittra, *Computational Methods for Electromagnetics* (IEEE, Piscataway, NJ, 1998).

<sup>13</sup>S. M. Rao, D. R. Wilton, and A. W. Glisson, *IEEE Trans. Antennas Propag.* **AP-30**, 409 (1982).

<sup>14</sup>G. R. Cowper, *Int. J. Numer. Methods Eng.*, 405 (1973).

<sup>15</sup>T. F. Eibert and V. Hansen, *IEEE Trans. Antennas Propag.* **AP-43**, 1499 (1995).

<sup>16</sup>E. Anderson, Z. Bai, C. Bischof, S. Blackford, J. Demmel, J. Dongarra, J. Du Croz, A. Greenbaum, S. Hammarling, A. McKenney, and D. Sorensen, *LAPACK Users' Guide*, 3rd ed. (SIAM, 1999).

<sup>17</sup>D. Yaghjian, *Antennas and Propagation Society, 2001 IEEE International Symposium*, 1999, Vol. 4, p. 2868.

<sup>18</sup>A. G. Fox and T. Li, *Bell Syst. Tech. J.* **40**, 458 (1961).

<sup>19</sup>K. Adam, D. A. Kaklamani, and N. K. Uzonoglu, *Antennas and Propagation Society, 1997 IEEE International Symposium*, 1999, Vol. 1, p. 302.

<sup>20</sup>A. Eriksson, P. Linnér, and S. Gevorgian, *IEE Proc.-Microw. Antennas Propag.*, 2001, Vol. 148, p. 51.

<sup>21</sup>M. C. Junger and D. Feit, *Sound, Structures, and their Interaction*, 2nd ed. (MIT Press, Cambridge, 1986).

<sup>22</sup>A. C. Ugural, *Stresses in Plates and Shells* (McGraw-Hill, New York, 1981).